Measurements of the surface thickness of liquid ^{4}He

1989 J. Phys.: Condens. Matter 1 289

(http://iopscience.iop.org/0953-8984/1/1/024)

J. Phys.: Condens. Matter **1** (1989) 289–297. Printed in the UK

Measurements of the surface thickness of liquid ^{4}He

D V Osborne
School of Physics, University of East Anglia, Norwich, UK

Received 21 March 1988

Abstract. Ellipsometric measurements of the thickness of the surface of liquid ^{4}He are reported for temperature from 1.4 to 2.3 K. The vertical thickness t within which the density changes from 90 to 10% of the bulk liquid density increases slightly with temperature from 1.4 to 2.1 K, having an average value of 9.4 Å at 1.8 K. There is some evidence of a rise of 2 or 3 Å between 2.1 K and the λ-point.

1. Introduction

At a liquid–vapour interface, the density $\rho(z)$ of a fluid does not change abruptly but changes continuously from liquid density to vapour density over a vertical distance of some ångströms. Following the ideas of Lekner and Henderson (1978a), it is convenient to define a surface thickness t as the difference in height between the point where the density is $\rho_1 + 0.9(\rho_2 - \rho_1)$ and the point where the density is $\rho_1 + 0.1(\rho_2 - \rho_1)$, ρ_1 and ρ_2 being the densities of bulk vapour and bulk liquid, respectively.

There have been measurements of t for a number of liquids (Rayleigh 1892, Raman and Ramdas 1927, Bouhet 1931, Beaglehole 1979, 1980), and recent x-ray techniques (Bosio and Oumezine 1984, Braslau *et al* 1985, Weiss *et al* 1986) may make it possible to determine not only the length scale but also the actual functional form $\rho(z)$ of the density profile. For a liquid helium surface, there have up to now been only one or two pieces of rather indirect experimental evidence about t (Echenique and Pendry 1976, Stern 1978), and no evidence about the shape of the profile. However, theorists have been interested in the question, and we list in table 1 some theoretical estimates of the length scale of the transition and of the surface tension emerging from the same calculations. Most of the calculations in table 1 refer to the liquid at absolute zero.

It is clear that there is a wide spread of predicted values of t—from 2.0 to 11.5 Å—and a fair range of predicted surface tensions. The latter predictions can be tested against the value of 0.374 mJ m^{-2} obtained by extrapolating the experimental values to absolute zero; it is the object of the present paper to present some experimental values of t to test theoretical predictions of this quantity.

2. Ellipsometry

Our type of ellipsometric measurement is based on the fact that, at the Brewster angle θ_B, the amplitude reflection coefficient r_p for light having its electric vector in the p

0953-8984/89/010289 + 09 $02.50

Table 1. Surface calculations for ^{4}He at $T = 0$ K. The asterisks indicate that the measured value of surface tension was used in calculating t. In the profile calculated by Mackie and Woo, $\rho(z)$ does not decrease monotonically as z increases.

Reference	Surface thickness t (Å)	Surface tension (mJ m^{-2})
Brouwer and Pathria (1967)	2.0	0.28
Fitts (1969)	11.5	*
Bowley (1970)	2.0	0.51
Shih and Woo (1973)	2.4	0.36
Chang and Cohen (1973)	4.5	0.40
Padmore and Cole (1974)	6.9	*
Liu *et al* (1975)	5.0	0.29
Ebner and Saam (1975)	7.8	0.38
Lekner and Henderson (1978b)	3.9	0.43
Mackie and Woo (1978)	—	0.33
Saarela *et al* (1983)	6.0	0.23
Pandharipande *et al* (1986)	7	0.40
Krotschek *et al* (1987)	About 6	—
Experiment	?	0.374

direction, i.e. in the plane of incidence, is exactly zero for an interface at which the refractive index changes discontinuously ($t = 0$). If the interface is diffuse rather than discontinuous, r_p attains a minimum but non-zero value at the Brewster angle, and this minimum value can be used to assess the extent to which the interface is spread. The optical quantity actually measured is the complex ratio r_p/r_s, where r_s is the amplitude reflection coefficient for light having its electric vector in the s direction, i.e. perpendicular to the plane of incidence.

In the present work, it is convenient to write

$$r_p/r_s \equiv c + id \equiv \rho_0 \exp(i\Delta_0) \tag{1}$$

where c, d, ρ_0 and Δ_0 are real. We work at angles θ of incidence within 0.01° of θ_B, which is 45.804° for a vapour–liquid helium surface. If we define $\varphi = \theta - \theta_B$, then it can be shown that, for $\varphi \ll 1$ and for $kt \ll 1$ (where $2\pi/k$ is the wavelength of the light), we have to a very good approximation

$$c = -\varphi(n_2^2 + n_1^2)^2/2n_2^3 n_1 \tag{2}$$

$$d = -k\eta(n_1^2 + n_2^2)^{1/2}/(n_1^2 - n_2^2). \tag{3}$$

Here η (Drude 1900) is defined by

$$\eta = \int \frac{(n^2 - n_1^2)(n^2 - n_2^2)}{n^2}\, dz \tag{4}$$

where $n(z)$ is the refractive index at height z and the integration extends from bulk liquid ($n = n_2$) up through the transition layer into the vapour ($n = n_1$). We see therefore that ellipsometric measurement of d enables us to deduce η which is a length characteristic of the thickness of the liquid–vapour interface. We note that, as the angle of incidence passes through θ_B ($\varphi = 0$), the real part of r_p/r_s goes through zero and changes sign while the imaginary part remains constant.

The 10–90% thickness t cannot be deduced directly from the measured η, but t can be estimated from η if a reasonable functional form for the variation of density $\rho(z)$ is assumed. In common with a number of other researchers, we use the hypothesis that $\rho(z)$ is a Fermi function and put

$$\rho(z) = \rho_1 + (\rho_2 - \rho_1)[1 + \exp(z/\delta)]^{-1}. \tag{5}$$

We also use the Clausius–Mossotti relation between $\varepsilon(z)$ and $\rho(z)$ and use $\varepsilon(z) = n^2(z)$. It can then be shown that

$$t = \delta \log 81 = 4.394\delta$$

and that

$$-\eta = \delta(\varepsilon_2 - \varepsilon_1)\log(\varepsilon_2/\varepsilon_1)$$

whence

$$t = -4.394\eta/(n_2^2 - n_1^2)\log(n_2^2/n_1^2). \tag{6}$$

3. The ellipsometer

The ellipsometer consists of two arms carrying optical components and pivoted about a common horizontal axis. The helium surface to be studied is contained in a cryostat placed so that the surface itself is situated at the axis of the ellipsometer. Light from the source passes down the first arm at the appropriate angle of incidence, is reflected at the helium surface and passes up the second arm to be detected. The angle of incidence is adjusted by moving both arms in a vertical plane, using screw jacks driven simultaneously from a common shaft. In this way the second arm is always in the right position to receive the reflected beam.

The ellipsometer and cryostat are shown diagrammatically in figures 1 and 2, respectively. The source of light for the ellipsometer is a 2 mW helium–neon laser L, giving out light of wavelength 633 nm and having its beam expanded to a diameter of 2.5 mm. The expander E is adjusted so that the beam waist is at the helium surface.

The Glan Thompson polariser P polarises the expanded beam so that its electric vector is close to the p direction. A Faraday rotator following the polariser can be used for fine adjustment of the polarisation direction. The rotator is also supplied with AC at frequency $\omega_1/2\pi = 70$ Hz to modulate the direction of polarisation with a peak-to-peak

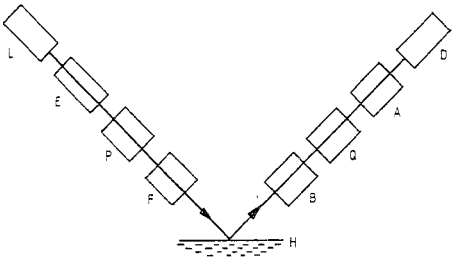

Figure 1. Elipsometer system: L, laser; E, beam expander; P, polariser; F, Faraday rotator; H, liquid-helium surface; B, birefringence modulator; Q, quarter-wave plate; A, analyser; D, detector (photomultiplier).

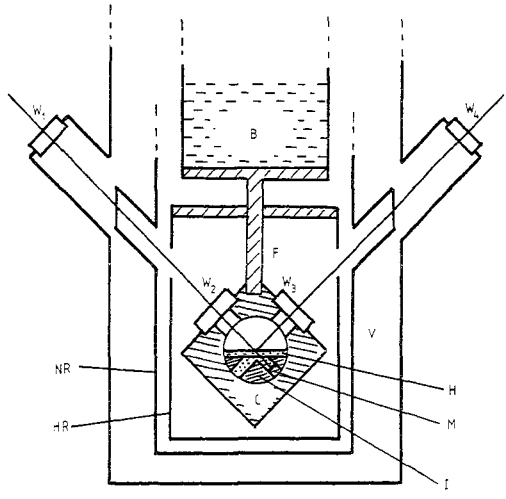

Figure 2. Schematic diagram of the cryostat: W_1, W_2, W_3, W_4, windows; C, copper chamber; H, liquid helium; I, brass insert; M, mirror; F, copper finger; B, main helium bath; V, thermal vacuum; NR, radiation shield at liquid-nitrogen temperature; HR, radiation shield at liquid-helium temperature.

amplitude $2P_1$ of about 0.0025 rad. This light passes into the cryostat through two windows of Schott SF57 glass, chosen because of its low birefringence even when under stress. The light beam is partially reflected at the liquid-helium surface and emerges from the cryostat through two further SF57 windows. After emerging, it passes through a photo-elastic modulator (Hinds International Inc. PEM 80) driven at frequency $\omega_2/2\pi$ = 50 kHz. This has the effect of varying the phase of the p component of the emerging beam with respect to its s component by a peak-to-peak phase amplitude $2\Delta_1$ chosen to be 2.16 rad. The modulator is followed by a quarter-wave plate Q having its fast axis at 45° to the p direction, and then a Glan Thompson analyser A driven by a stepping motor and gearing with a resolution of 0.01°. The light passing through the analyser is incident on a photomultiplier, the output from which is taken to a current amplifier.

Sufficient detail of the cryostat is shown in figure 2 to make it clear that the helium surface under study is that of a small sample condensed into a chamber C cooled by the main helium bath B by conduction along the copper finger F. The helium forms a shallow pool in a cylindrical cavity having its axis horizontal. The lower part of the cavity is occupied by a brass insert I having two blind holes at 45° to the vertical. That fraction of the incident beam intensity which is transmitted through the helium surface, i.e. the great majority of it, strikes a mirror M at the bottom of the first hole and is reflected back in the general direction of the incident beam. This prevents it from being absorbed in the chamber and causing possible heat currents. The second hole forms a recess which reduces any possible scattered light emerging towards the detector. The shallowness of the helium pool (about $\frac{1}{2}$ mm, except over the central hole) enables the viscosity of the normal component to help to damp out accidental disturbances of the surface.

I am indebted to Professor M B Glauert (1987) for a reassuring discussion of the shape of a liquid surface under the influence of surface tension when the surface is bounded by a rectangle of vertical walls, as in this case. It is clear from his calculations that a 1.8 cm square helium surface has a central region of 6 mm square within which the slope of the surface departs from horizontal by less than 2×10^{-6} rad. The centre part of the surface is therefore very satisfactorily flat for our beam diameter of 2.5 mm.

The intensity I falling on the photomultiplier contains a time-independent contribution and harmonics and combination tones of ω_1 and ω_2, each contribution having a magnitude which depends on the angle of incidence. The most useful component to isolate is the cross term

$$I_{12} = 2A^2 r_s^2 \rho_0 J_1(\Delta_1) P_1 \sin(2a - \Delta_0) \cos(\omega_1 t) \cos(\omega_2 t) \tag{7}$$

where A is the amplitude of the incident light and a is the angle between the pass direction of the analyser and the slow direction of the quarter-wave plate. To measure the amplitude of I_{12}, the signal from the photomultiplier is taken through the current amplifier to a phase-sensitive detector having a reference signal driven from the photoelastic modulator at frequency ω_2 (50 kHz) and having a response time of the order of 10^{-3} s. The output of this detector contains, *inter alia*, a component of frequency ω_1 (70 Hz) proportional to the amplitude of I_{12}. This output is taken to a second phase-sensitive detector referenced to ω_1 and the DC output emerging from the second detector is proportional to the amplitude of I_{12}.

If we now choose to set the analyser angle to one of the specific values $a = -\pi/4, 0, +\pi/4, +\pi/2$, we find from equations (1) and (7) that

$$V_{12} = \pm K\varphi(n_2^2 + n_1^2)^2/2n_1 n_2^3 \qquad (a = \pm\pi/4) \tag{8}$$

or

$$V_{12} = \mp Kk\eta(n_1^2 + n_2^2)^{1/2}/(n_1^2 - n_2^2) \qquad (a = 0, \pi/2) \tag{9}$$

where V_{12} is the voltage output proportional to the intensity I_{12} and K is a constant involving the input intensity, amplifier gains and a number of other quantities which do not depend on the angle of incidence. These measurements of V_{12} therefore offer a direct method of determining the real and imaginary parts of r_p/r_s (see equations (1)–(3)). To determine η, we first set $a = \pm\pi/4$ and measure V_{12} for a modest range of φ, thereby enabling K to be found. We then set a equal to 0 and then to $\pi/2$, and the difference between these readings of V_{12} enables η to be determined since K is now known.

Note that V_{12} is either linearly related to φ (equation (8)) or independent of it (equation (9)). If therefore φ has small fluctuations due to disturbances of the liquid surface, the measured time average of V_{12} is the value corresponding to the time average of φ, as required.

φ, it will be remembered, is the departure of the angle θ of incidence from the Brewster angle θ_B. φ is adjusted by means of the screw jacks controlling the ellipsometer arms, and the change in φ is determined by means of a dial gauge recording the movement of one arm. A typical range of φ used is from -10^{-4} rad to $+10^{-4}$ rad (dial gauge $\pm$ 0.003″ at a radius of 33″).

The temperature of the helium sample is determined from its vapour pressure using a gauge situated at the top of the condensing line. Above the λ-point the sample temperature tends to sit about 80 mK above the bath temperature which, at present, makes it impossible to obtain readings between T_λ and 2.26 K.

4. Results

Experiments were conducted at temperatures between 1.400 and 2.295 K. As predicted in equations (8) and (9), V_{12} was independent of φ with $a = 0$ or $\pi/2$ and was proportional to φ with $a = \pm\pi/4$. Values of η were calculated from the V_{12} measurements using

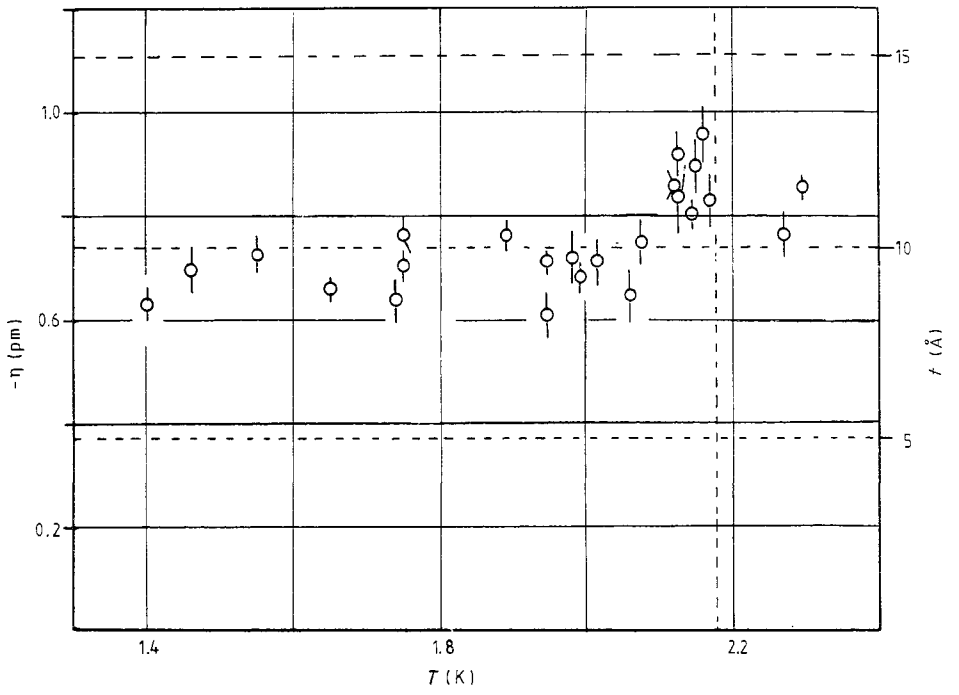

Figure 3. Surface thickness of liquid ^{4}He; the left-hand ordinate scale is the directly measured $-\eta$ in picometres; the right-hand scale is the 10–90% surface thickness t in ångströms, assuming a Fermi function density profile.

equations (8) and (9), and adopting the refractive indices measured by Edwards (1957, 1958). The results for η as a function of T are shown in figure 3; the ordinate scale for η is shown on the left. The error bars are standard deviations estimated from the straight lines of equation (9) and from the fluctuations of the 'constant' V_{12} of equation (8). Hypothetical values of t have been deduced using equation (6); the denominator in that expression varies by only 3 parts in 10^3 over the temperature range used and so, within the modest experimental accuracy claimed, $t = 1353\eta$ at all temperatures. t can therefore be read from the same graph as η, using the ordinate scale shown on the right.

From 1.4 to 2.1 K, η and t do not vary strongly with temperature. The centroid of these 15 points gives $t = 9.36$ Å at $T = 1.813$ K. If a linear fit be attempted by least squares, the result is a slope of 0.49 ± 0.82 Å K^{-1} and an intercept at $T = 0$ K of 8.5 ± 1.5 Å. t appears to rise by 2–3 Å as T approaches T_λ closely, but the experimental accuracy is not at present good enough to give any details of this rise. The only two measurements so far made above T_λ suggest that the surface thickness of liquid helium I is not remarkably different from that of liquid helium II.

Some researchers (see, e.g., Beaglehole 1979, 1980, Bouhet 1931) who have made ellipsometric measurements on liquid surfaces have described their results in terms of the ellipticity $\bar{\rho}$ of the surfaces. $\bar{\rho}$ is the value of ρ (see equation (1)) exactly at the Brewster angle and is related to η by

$$\bar{\rho} = \tfrac{1}{2}[(n_1^2 + n_2^2)^{1/2}/(n_1^2 - n_2^2)]\, k\eta. \tag{10}$$

By way of example, our typical value of $\eta = -0.70$ pm corresponds to $\bar{\rho} = 8.6 \times 10^{-5}$ at the wavelength of 633 nm used in our experiments.

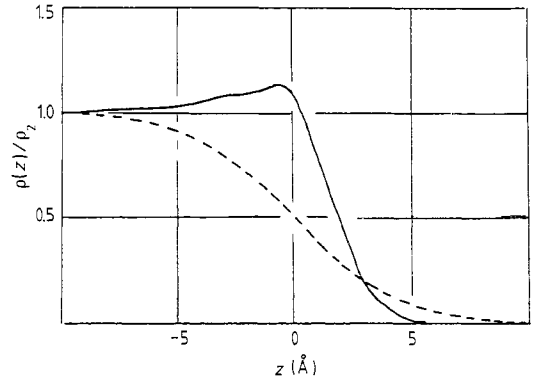

Figure 4. Theoretical density profiles of the liquid-helium surface: ——, Mackie and Woo (1978); – – –, Fermi function.

5. Discussion

5.1. Functional form of $\rho(z)$

It must be emphasised that the values of $-\eta$ (see equation (4)) in figure 3 are the result of measurement, but the corresponding values of t are conjectural, depending as they do on the hypothesis that $\rho(z)$ is a Fermi function. For the value of t at the centroid of the lowest 15 points (i.e. $t = 9.36$ Å at $T = 1.813$ K), the particular Fermi function is that shown by the broken line in figure 4 in which $\rho(z)/\rho_2$ is plotted against z, where ρ_2 is the bulk liquid density. For such a function, every part of the curve makes a negative contribution to the integral for η (equation (4)), the major contribution coming from the central region around $z = 0, \rho(z)/\rho_2 = \frac{1}{2}$. As can be seen from figure 3, this particular Fermi function corresponds to $\eta = -0.69$ pm.

It is interesting to contrast this with the consequences of a non-monotonic profile such as that calculated on theoretical grounds by Mackie and Woo (1978). This profile is shown as a full line in figure 4. Equation (4) can be used to calculate what η would be for this profile. It is convenient to split the range of integration into two parts and to obtain

$$\eta = \eta_1 + \eta_2 = \int_{-\infty}^{0} \frac{(n^2 - n_1^2)(n^2 - n_2^2)}{n^2}\,\mathrm{d}z + \int_{0}^{+\infty} \frac{(n^2 - n_1^2)(n^2 - n_2^2)}{n^2}\,\mathrm{d}z$$

$$= +0.179\ \text{pm} - 0.209\ \text{pm} = -0.030\ \text{pm}.$$

We see that their relatively modest overshoot, with a maximum density 1.12 times the bulk liquid density, gives a very large positive contribution to η for $z < 0$, only just outweighed by the negative contribution from $z > 0$. If our large measured value of $\eta = -0.69$ pm were the result not of a monotonic Fermi function but of near cancellation between a negative contribution at $z > 0$ and a positive contribution from a density overshoot at $z < 0$, then this would imply a profile spread out over a distance of some hundreds of ångtroms. Such a very gradual profile seems improbable, and we therefore believe that the general size of our values of η strongly suggests a monotonic decrease in ρ as z increases.

5.2. Theoretical predictions of the surface thickness

Referring to table 1, we see that most calculations predict a value of t considerably smaller than the trend shown in figure 3. The most successful work would appear to be that of Ebner and Saam (1975) which leads to reasonably accurate predictions of both t and γ starting from the pair potential and using a density-functional theory.

5.3. Temperature dependence of η

Our measurements show a barely significant increase in η with temperature in the range 1.4–2.1 K. Some increase would be expected, since thermal fluctuations of the surface level have a mean square amplitude proportional to T, and these will contribute to the total surface thickness. A number of calculations of these fluctuations have been carried out (see, e.g., Buff *et al* 1965, Cole 1980, Vrij *et al* 1981, Marvin and Toigo 1982), and some recent work (see, e.g., Krotschek *et al* 1987) treats the problems of surface structure and of surface excitations as a whole. Simple models suggest that the fluctuations, in so far as they can reasonably be calculated independently of the structure, make a rather small contribution to the measurable surface thickness. This agrees qualitatively with our observed very weak temperature dependence, but neither theory nor our experiments are yet sufficiently reliable for any quantitative discussion of this dependence to be useful.

Acknowledgments

I gratefully acknowledge the assistance of Dr C L Riddiford who largely designed the ellipsometer, and I am indebted to Professor M B Glauert for a discussion of the liquid meniscus shape. I am grateful for the generous technical help of Mr B Hart, Mr A Harwood, Mr C Hindle, Mr G Plain, Mr D Woodcock, and Mr C A Wright who between them built, assembled and modified the ellipsometer and its electronics and provided the liquid helium. I also acknowledge the receipt of a Research Grant from the Science and Engineering Research Council which enabled this work to be started.

References

Beaglehole D 1979 *Phys. Rev. Lett.* **43** 2016–8
—— 1980 *Physica* B **100** 163–74
Bosio L and Oumezine M 1984 *J. Chem. Phys.* **80** 959–60
Bouhet C 1931 *Ann. Phys., Paris* **15** 5–130
Bowley R M 1970 *J. Phys. C: Solid State Phys.* **3** 2012–9
Braslau A, Deutsch M, Pershan P S, Weiss A H, Als-Nielsen J and Bohr J 1985 *Phys. Rev. Lett.* **54** 114–7
Brouwer W and Pathria R K 1967 *Phys. Rev.* **163** 200–5
Buff F P, Lovett R A and Stillinger F H Jr 1965 *Phys. Rev. Lett.* **15** 621–3
Chang C C and Cohen M 1973 *Phys. Rev.* A **8** 1930–6
Cole M W 1980 *J. Chem. Phys.* **73** 4012–4
Drude P 1900 *Theory of Optics* (Transl 1959: New York: Dover)
Ebner C and Saam W F 1975 *Phys. Rev.* B **12** 923–39
Echenique P M and Pendry J B 1976 *Phys. Rev. Lett.* **37** 561–3
Edwards M H 1957 *Phys. Rev.* **108** 1243–5
—— 1958 *Can. J. Phys.* **36** 884–97

Fitts D D 1969 *Physica* **42** 205–12
Glauert M B 1987 private communication
Krotschek E, Stringari S and Treiner J 1987 *Phys. Rev.* B **35** 4754–63
Lekner J and Henderson J R 1978a *Physica* A **94** 545–58
—— 1978b *J. Low Temp. Phys.* **31** 763–84
Liu K S, Kalos M H and Chester G V 1975 *Phys. Rev.* B **12** 1715–9
Mackie F D and Woo C-W 1978 *Phys. Rev.* B **18** 529–35
Marvin A M and Toigo F 1982 *Phys. Rev.* A **26** 2927–39
Padmore T C and Cole M W 1974 *Phys. Rev.* A **9** 802–7
Pandharipande V R, Piper S C and Wiringa R B 1986 *Phys. Rev.* B **34** 4571–82
Raman C V and Ramdas L A 1927 *Phil. Mag.* **3** 220–3
Rayleigh Lord 1892 *Phil. Mag.* **33** 1–19
Saarela M, Pietiläinen P and Kallio A 1983 *Phys. Rev.* B **27** 231–40
Shih Y M and Woo C-W 1973 *Phys. Rev. Lett.* **30** 478–81
Stern F 1978 *Phys. Rev.* B **17** 5009–15
Vrij A, Joosten J G H and Fijnaut H M 1981 *Adv. Chem. Phys.* **48** 329–96
Weiss A H, Deutsch M, Braslau A, Ocko B M and Pershan P S 1986 *Rev. Sci. Instrum.* **57** 2554–9